HHS Public Access

Author manuscript

Nat Commun. Author manuscript; available in PMC 2015 July 30.

Published in final edited form as:

Nat Commun. ; 6: 6170. doi:10.1038/ncomms7170.

NR2F1 controls tumor cell dormancy *via* SOX9 and RARβ driven quiescence programs

Maria Soledad Sosa[1], **Falguni Parikh**[1,2], **Alexandre Gaspar Maia**[3], **Yeriel Estrada**[1], **Almudena Bosch**[1], **Paloma Bragado**[1], **Esther Ekpin**[1], **Ajish George**[1], **Yang Zheng**[2], **Hung-Ming Lam**[6], **Colm Morrissey**[6], **Chi-Yeh Chung**[3], **Eduardo F. Farias**[1,4], **Emily Bernstein**[3,4,5], and **Julio A. Aguirre-Ghiso**[1,2,4,5,*]

[1]Division of Hematology and Oncology, Department of Medicine, Mount Sinai School of Medicine, New York, NY 10029

[2]Department of Otolaryngology, Mount Sinai School of Medicine, New York, NY 10029

[3]Department of Oncological Sciences, Mount Sinai School of Medicine, New York, NY 10029

[4]Tisch Cancer Institute, Mount Sinai School of Medicine, New York, NY 10029

[5]Black Family Stem Cell Institute, Mount Sinai School of Medicine, New York, NY 10029

[6]Department of Urology, University of Washington, Seattle, WA

Abstract

Metastases can originate from disseminated tumor cells (DTCs), which may be dormant for years before reactivation. Here we find that the orphan nuclear receptor NR2F1 is epigenetically upregulated in experimental HNSCC dormancy models and in DTCs from prostate cancer patients carrying dormant disease for 7–18 years. NR2F1-dependent dormancy is recapitulated by a co-treatment with the DNA demethylating agent 5-Aza-C and retinoic acid across various cancer types. NR2F1-induced quiescence is dependent on SOX9, RARβ and CDK inhibitors. Intriguingly, NR2F1 induces global chromatin repression and the pluripotency gene *NANOG*, which contributes to dormancy of DTCs in the bone marrow. When NR2F1 is blocked *in vivo*, growth arrest or survival of dormant DTCs is interrupted in different organs. We conclude that

*Correspondence to: Julio A. Aguirre-Ghiso, Division of Hematology and Oncology, Department of Medicine, Head and Neck Cancer Research Program, Department of Otolaryngology, Mount Sinai School of Medicine, New York, NY, 10029. Phone: 212-241-9582 Fax: 212-241-4096 Box: 1079 julio.aguirre-ghiso@mssm.edu.

Author contributions: MSS: designed and optimized experimental approach and performed in vitro and in vivo experiments, analyzed data and co-wrote the manuscript, FP: performed experiments, AGM: performed ChIP-QPCR experiments, YE: performed in vivo experiments, AB: performed in vivo experiments, PB: performed cell biology experiments, EE: performed cell biology experiments. AG: performed computational analysis, YZ: performed QPCR experiments; HML: performed human DTC expression profiling experiments and analysis, CM: performed human DTC expression profiling experiments and analysis, CYC: performed cell biology experiments, EFF: performed mouse experiments, provided general guidance and oversight, analyzed data and co-wrote the manuscript, EB: designed and optimized experimental approach, provided general guidance and oversight, analyzed data and co-wrote the manuscript, JAA-G: designed and optimized experimental approach, provided general guidance and oversight, analyzed data and co-wrote the manuscript.

Conflict of interest. The authors declare no competing financial interests..

Accession codes: Gene Expression Omnibus under the accession number GSE58588 and GSE48995.

NR2F1 is a critical node in dormancy induction and maintenance by integrating epigenetic programs of quiescence and survival in DTCs.

INTRODUCTION

A large proportion of patients diagnosed with cancer harbor non-proliferative residual tumor cells, which can fuel incurable local or distant recurrences[1]. The ability of dormant residual tumor cells to persist but also interconvert between dormancy and proliferation may be the result of epigenetic reprogramming mechanisms[2]. However, mechanisms and markers that identify dormant cells at risk of resuming growth are unavailable. We reported that p38α/β regulates a quiescence transcription factor (TF) network that contains proliferation/growth arrest and pluripotency/self-renewal genes [3,4,5]. The p38α/β pathway and quiescence were activated by TGFβ2 signaling specifically in disseminated tumor cells (DTCs) that are dormant in the bone marrow[6]. Further the p38α/β-regulated TF network served as a "dormancy signature" that was enriched in estrogen receptor (ER) positive luminal over ER-negative basal-type primary breast tumors[7] and predicted for longer metastasis-free periods in the ER+ group[7]. Thus, we hypothesized that genes within this signature may influence the timing of metastasis *via* regulation of dormancy.

Among the genes in the dormancy signature[3,6,7] we identified NR2F1, an orphan nuclear receptor [8] that induces cell lineage determination in response to signals like retinoic acid (RA) [9], limits iPS reprogramming [4] and regulates enhancer elements during human neural crest cell differentiation [10]. Because these processes regulate pluripotency and limit proliferation we investigated whether NR2F1 and these processes were linked to the interconversion between cancer cell dormancy and proliferation.

Like other genes in the RA pathway (e.g. RARβ) [11] NR2F1 mRNA is downregulated in several cancers including HNSCC, prostate, lung and breast vs. normal tissues (Oncomine database)[12–16] and it is functionally linked to a breast cancer susceptibility locus (Mcs1)[17]. Further, upregulation of NR2F1 correlated with longer disease-free periods after hormonal ablation in prostate cancer[18]. Thus, changes in NR2F1 levels in primary tumors may influence residual tumor cell fate.

Here we provide evidence that NR2F1 coordinates gene expression found in quiescent cells and also in self-renewing ES cells[19]. We show that NR2F1 regulates the behavior of residual tumor cells in post-operative mice as its inactivation causes a rapid switch from dormancy to proliferation of occult tumor cells and systemic recurrence. This is true except in the bone marrow, where NR2F1 appears to regulate DTC survival. Importantly, restoration of NR2F1 expression using DNA demethylating agents and activation of RA signaling is sufficient to recapitulate the quiescence program and induce chromatin changes linked to a durable dormant state. These findings break new ground in our understanding of the dormancy mechanisms and identify markers that might pinpoint residual cancer with the ability to escape dormancy.

RESULTS

NR2F1^{high} human tumor cells are dormant

We first used the squamous cell carcinoma cell line HEp3 model of proliferation vs. dormancy to dissect the molecular mechanisms of conversion of malignant cells into a dormancy-like behavior characterized by tumor cell quiescence[3, 6, 20–25]. Proliferating (T-HEp3) cells obtained from tumors and kept in culture reprogram into a dormant/quiescent phenotype (D-HEp3 cells) after prolonged passaging in vitro. However, this dormant phenotype is not manifested *in vitro* but it is observed only after injection of D-HEp3 cells *in vivo* in nude mice s.c. or in the chicken embryo chorioallantoic membrane (CAM). In these in vivo settings the dormant phenotype of D-HEp3 cells can persist for months before reactivation[3, 6, 20, 26]. We compared the expression profiles of deeply quiescent D-HEp3 cells that form small nodules that do not change in size in vivo or proliferative T-HEp3 cells that form growing tumor masses *in vivo* [3, 20] and found that NR2F1 was induced ~3 fold in the former cells (Fig. 1a – see also methods for access to full expression profiles). This was corroborated by immunohistochemistry (IHC), immunofluorescence (IF) (Fig. 1b, Supplementary Fig. 1a) and WB, where nuclear NR2F1 protein was 3–4 folds higher in D-HEp3 cells than in T-HEp3 cells (Fig. 1b). This was also true for other genes in the RA pathway (RARβ) [27] (Fig. 1a, Supplementary 1b). In two additional aggressive HNSCC cell lines, FaDu and SQ20B [28], NR2F1 protein and mRNA levels were barely detectable (Fig. 1b). Thus, NR2F1 is downregulated in T-HEp3, FaDu and SQ20B HNSCC cells *in vitro* and tumors *in vivo* (T-HEp3) when compared to dormant D-HEp3 cells *in vitro* and dormant nodules *in vivo*.

To determine the function of NR2F1 in quiescent D-HEp3 cells *in vivo* [3] we performed NR2F1 knockdown *via* siRNA and found that NR2F1 promoted D-HEp3 cell exit from dormancy and tumor growth, comparable to a siRNA to p38α, as shown for other TFs in the p38α/β regulated network[3, 6] (Fig. 1d, Supplementary Fig. 1c); no differences were observed in potency of phenotype between siNR2F1 and sip38α. Exit from dormancy coincided with downregulation of cell cycle inhibitors such as p16, p27, p15 and HES-1, all genes involved in quiescence [29, 30] (Fig. 1e). Further, NR2F1 depletion also induced upregulation of cyclinD1 levels and Ki67 staining indicative of G0 exit.

To test the potential human implications of these findings we next tested whether NR2F1 was re-expressed in prostate cancer DTCs[31]. We chose prostate cancer because this cancer type is known to undergo prolonged dormancy phases and because NR2F1 is commonly downregulated in prostate primary tumors[15, 16], but may become upregulated after hormonal ablation, which is thought to lead to residual disease dormancy[18]. To this end we compared individual prostate cancer DTCs isolated *via* EpCAM marking from the bone marrow of post-radical prostatectomy patients with no evidence of disease (NED – dormant disease) or advanced proliferative disease (ADV). NED patients showed undetectable PSA level (<0.1ng/mL) 7–18 years after prostatectomy. ADV patients showed disease progression with failed treatment or existing distant metastasis. Seven EpCAM+ individual NED cells (4 patients) and 37 ADV cells (6 patients) were processed for expression profiling as indicated in Table I and Experimental Procedures[31]. When comparing NED vs. ADV PCa DTCs we

found that 42.8% of NED DTCs showed NR2F1 upregulation vs. 10.3% in ADV patient-derived DTCs (Fig. 1c). The average mRNA levels for NR2F1 showed a trend towards upregulation ($p<0.08$) in NED vs. the ADV patient derived DTCs (Fig. 1c). A significant difference in mRNA levels ($p<0.0117$) was found for TGFβ2[6] another dormancy gene we recently linked to BM DTC dormancy that was also more frequently upregulated in NED vs. ADV DTCs (42.8% NED vs. 18% ADV) (Fig. 1c). We conclude that dormancy genes found upregulated in HNSCC experimental models (this study and[6]) are also found upregulated in DTCs from PCa patients carrying dormant disease.

Epigenetic regulation of NR2F1 expression

IHC analysis showed that compared to benign adjacent oral mucosa NR2F1 expression was absent or low in primary (n=15) or recurrent (n=9) HNSCC tumors (Fig. 2a and Supplementary Fig. 1d and e) and patient-matched lymph node metastases (n=11) (Fig. 2a). Further, while 27% of squamous cells in benign adjacent tissues were $NR2F1^{high}$ (7–66% range), only $1.5\pm2.5\%$ of tumor cells in primary and recurrent lesions were $NR2F1^{high}$. These results show that overall NR2F1 is downregulated in tumor tissues and the intratumor heterogeneity of expression is very low (Fig. 2a and Supplementary Fig. 1d and e). Primary tumor tissues showed that 67% of the tumor cells were Ki67+ and none expressed NR2F1, suggesting that proliferative tumor cells are negative for NR2F1. (Supplementary Fig. 1e). The overall downregulation of NR2F1 in tumor vs. normal squamous tissues is in accord with the expression profiling study[12] where NR2F1 was downregulated in ~85% (n=41) of HNSCC primary tumors and in ~86% (n=16) local recurrences. NR2F1 mRNA and protein levels were also lower in human breast carcinoma tissues and in the breast tissue of 20 week-old MMTV-Neu and -Myc mice (Supplementary Fig. 2a–c), which at this age develop pre-malignant ADH and DCIS-like lesions[32]. Further, in at least three studies[13, 33, 34] including the breast cancer TCGA showed that in ~80% tumor samples NR2F1 was significantly downregulated vs. normal tissue (e.g., $p<1.06\times10^{-25}$ - TGCA data as measured using a t-Test – Oncomine source).

We next tested whether NR2F1 might be downregulated by DNA promoter methylation. Treatment of T-HEp3 and FaDu cells that express negligible levels of NR2F1 with 5-aza-Deoxycytidine (5-Aza-C), strongly increased NR2F1 mRNA expression by >3 fold without any toxicity (Fig. 2b and Supplementary Fig. 2d). However, analysis of DNA promoter methylation showed no differences in CpG island methylation between T-HEp3 and D-HEp3 cells (Supplementary Fig. 2e). ChIP analysis covering a region spanning −10Kb to +3Kb of the transcription start site (TSS) of the NR2F1 gene revealed that the H3K4me3 and H3K27ac transcriptional activation marks are highly enriched at the NR2F1 TSS in D-HEp3 as compared to T-HEp3 cells (Fig. 2c). In contrast, the H3K27me3 repressive mark was enriched in the promoter of NR2F1 in T-HEp3 cells (Fig. 2c). These changes in H3-PTMs correlated with the NR2F1 mRNA levels in T- vs. D-HEp3 HNSCC cells. ChIP analysis for the same H3-PTMs mentioned above in D-HEp3 cells with and without NR2F1 knock down showed that on its own promoter at least H3K4me3 seems to be regulated by NR2F1 (+1 position) (Fig. 2d). We conclude that DNA promoter methylation in regions not covered by our analysis and/or changes in histone-H3 PTMs and transcriptional activation, contribute to NR2F1 silencing in proliferative T-HEp3 cells.

NR2F1 regulates SOX9 and RARβ during dormancy

TF network analysis of gene profiles regulated by p38α/β[3] identified 40 co-regulated genes with predicted or validated binding elements for NR2F1 in their promoters (Supplementary Fig. 3a, Table II). Ten of these genes contained both NR2F1 and RARβ (a target of NR2F1[35]) binding sites. These genes were upregulated >2.8 fold in D-HEp3 cells both in culture and *in vivo* (Figs. 3a - 1a). We focused on SOX9, because its promoter is bound by NR2F1 and RARβ[10] and it is a RA- and p38α/β-responsive TF[36,3] linked to growth inhibition and differentiation[37]. Accordingly, overexpression in T-HEp3 cells with an active MKK6 mutant (p38 activator), upregulated SOX9, NR2F1 and RARβ mRNAs (Supplementary Fig. 3b). Further, NR2F1 overexpression in T-HEp3 cells greatly increased the activity of a SOX9-luciferase reporter (Supplementary Fig. 3c) suggesting that SOX9 is a direct target of NR2F1. Finally, we show that as in Fig. 2c knock down of NR2F1 reduced the presence of H3K4me3 marks in the promoters of SOX9 and RARβ in dormant D-HEp3 cells (Supplementary Fig. 3d) without affecting H3K27me3 marks in any tested promoter (not shown). Thus, NR2F1 is in part responsible for inducing active transcription H3-PTMs in its own promoter and that of its target genes (Supplementary Fig. 3d).

NR2F1 overexpression mimicked dormancy in T-HEp3 cells, as it induced growth suppression a reduction in Ki-67 levels and induction of p27 and SOX9 proteins and p16 and SOX9 mRNAs (Fig. 3b–c, Supplementary Fig. 3e). Importantly, SOX9 was required for NR2F1-induced quiescence as RNAi to SOX9 in T-HEp3 cells completely blocked NR2F1-dependent induction of growth suppression (Fig. 3c). This was accompanied by a decrease in p16 levels (Fig. 3c). RNAi to SOX9 in vector transfected tumor cells also stimulated tumor growth suggesting that basal NR2F1 expression negatively regulates T-HEp3 proliferation. A siRNA against SOX9 in D-HEp3 cells also promoted tumor growth and decreased p16 and p27 mRNA levels and p27 protein levels (Fig. 3d, Supplementary Fig. 3f), but no changes were observed in p15 and HES-1 levels (not shown) (Fig. 3d). SOX9 was sufficient to induce dormancy because overexpression of a cDNA encoding human SOX9 completely reversed the pro-proliferative effects of NR2F1 siRNA on D-HEp3 cells (Fig. 3e).

Since RA regulates NR2F1 expression[38], we tested whether the pan-RAR ligand atRA, increased NR2F1 and its target genes. We found that RARβ, SOX9 and NR2F1 itself were induced between 1.3–4 fold in T-HEp3 and FaDu cells, in response to 48h treatment with atRA (Fig. 4a and Supplementary Fig. 4a). NR2F1 depletion in T-HEp3 cells reduced atRA-induced upregulation of RARβ and SOX9 and even basal levels of SOX9 were further reduced upon NR2F1 and RARβ knock down (Supplementary Fig. 4b).

We next explored the effect of 5-AzaC on NR2F1 induction of target genes. Both RARβ and SOX9 induction in T-HEp3 and FaDu cells was strongly enhanced by the treatment (Supplementary Figs.4c and 4d). Interestingly, NR2F1 overexpression was not sufficient to upregulate RARβ mRNA (Supplementary Fig. 4e) but pretreatment with 5-Aza-C followed by NR2F1 overexpression now made the T-HEp3 cells permissive to RARβ upregulation by exogenous NR2F1 above the effect of 5-Aza-C alone (Supplementary Fig. 4e). Accordingly, in T-HEp3 cells treated with a combination of low-dose of Aza-C (5nM) + atRA

(Supplementary Fig. 4f), NR2F1, SOX9 and RARβ mRNAs were significantly upregulated (Fig. 4a).

The effect of atRA on RARβ was transient and its expression returned to pre-induction levels 3 days after atRA wash out (Fig. 4b). In contrast, when cells were pre-treated with AzaC (5 nM) followed by atRA (2 μM), the induced levels of RARβ were maintained even after atRA removal for 3 days (Fig. 4b). The AzaC + atRA treatment was also able to induce RARβ expression across various cancer cell line subtypes (Supplementary Fig. 5a). Importantly, the sustained expression of RARβ in these conditions required NR2F1 expression as tested in T-HEp3, MCF7 and SQ20B cells (Fig. 4c and Supplementary Fig. 5a). These results argue that in carcinoma cell lines from different tissues, AzaC-plus-atRA induced gene expression is durable and dependent on NR2F1.

AtRA and 5-Aza-C treatment induces NR2F1-dependent dormancy

To expand the above experiments, we queried whether treatment of T-HEp3 cells with atRA would induce key hallmarks of reprogramming into quiescence *in vivo*. Treatment with atRA for 5 days resulted in inhibition of tumor growth *in vivo* using the chicken chorioallantoic membrane assays for rapid *in vivo* readout[20] (Fig. 4d). Growth inhibition was with no apparent change in apoptosis or senescence (Supplementary Fig. 5b). Analysis of the tumor tissue from CAMs showed that atRA treatment caused a marked upregulation of dormancy genes. These included upregulation of RARβ and p21 mRNAs and NR2F1 and SOX9 proteins (Fig. 4e) and downregulation of Ki67 and P-ERK1/2 levels (Fig. 4e), suggesting a G0-arrest. Treatment with atRA also increased the phosphorylation of ATF2, a downstream p38 target (Fig. 4e) suggesting a low ERK/p38 activity ratio[20]. Importantly, in T-HEp3 cells RNAi to SOX9 and NR2F1 was sufficient to eliminate the growth inhibitory effect of atRA *in vivo* (Fig. 4f). However, as expected (Fig. 4b), atRA-treated T-HEp3 cells that were growth inhibited for one week, escaped this inhibition by atRA after a second week *in vivo* (Supplementary Fig. 5c).

We next tested whether the persistent effect of combined 5-Aza-C+atRA treatment in culture (Fig. 4b), could induce prolonged T-HEp3 quiescence state *in vivo*. We used a Tet-ON inducible H2B-GFP-tagged T-HEp3 line where doxycycline (DOX) induces H2B-GFP and upon de-induction and DNA replication only cells that are quiescent are H2B-GFP positive. H2B-GFP-tagged T-HEp3 cells treated only *in vitro* with 5-Aza-C+atRA for 4 days were then followed on CAMs for 6 days (Fig. 4g). In this sequence the 5-Aza-C+atRA treatment induced a persistent dormant phenotype that lasted for at least 2 weeks in vivo (Supplementary Fig. 5d). This correlated with the percentage of H2B-GFP positive cells in AzaC+atRA-treated cells that was ~5-fold greater at 6 days than in vehicle treated-cells (Fig. 4g). Together these data argue that restoring NR2F1, RARβ and SOX9 expression during the AzaC+atRA reprogramming phase could induce a sustained (at least 2 weeks) dormant phenotype.

NR2F1 regulates expression of pluripotency genes

NR2F1 regulates lineage commitment and differentiation [10] and it was shown to block iPS reprogramming [4]. However, whether NR2F1 affects pluripotency gene expression upon

dormancy onset is unknown. We found that, both NANOG and SOX2 mRNAs were significantly upregulated in dormant BM-HEp3[6] and D-HEp3 cells over the proliferative T-HEp3 and Lu-HEp3[6] cells (Fig. 5 a). Furthermore, NANOG and SOX2 mRNAs were strongly induced by the AzaC+atRA treatment and siRNAs to NR2F1 completely eliminated this induction (Fig. 5b). The induction of these pluripotency genes by the Aza+atRA reprogramming protocol was not correlated with tumor initiating capacity as this reprogramming inhibited the ability of T-HEp3 cells to form tumor spheres in stem cell media (Supplementary Fig. 5e). NR2F1 also inhibited tumor growth of MMTV-Myc mammary tumors cells, where overexpression of NR2F1 significantly reduced tumorigenicity in mice and tumor sphere formation (Fig. 5c–d and Supplementary Fig. 6a). We conclude that induction of pluripotency genes by NR2F1 in dormant cancer cells is associated with a growth suppressive or quiescent behavior and not with immediate tumor initiating capacity.

NR2F1^{high} cells display a global repressive chromatin state

We showed that tumor initiating cells (TICs) display an open chromatin state (H3K27me3^{low}, H3K9me3^{low,} H3K4me3^{low}), while non-tumor initiating cells (NTICs) displayed a reverse profile and a more repressive or “bivalent” chromatin state[28]. NR2F1 could regulate local changes in H3-PTMs in its own and SOX9 and RARβ promoters but the global effect of NR2F1 on chromatin marks was not obvious. IHC and IF analysis showed that in contrast to T-HEp3 cells (NR2F1^{low}), D-HEp3 cells (NR2F1^{high}) showed a H3K9me3^{high} and H3K27me3^{high} profile (Fig. 6a). Accordingly, the AzaC+atRA reprogramming protocol rendered T-HEp3 cells H3K27me3^{high}/H3K9me3^{high}/ H3K4me3^{low}/NR2F1^{high}/SOX9^{high} and quiescent *in vivo* (Fig. 6b-c, Supplementary Fig. 5d, Supplementary Fig. 6b, Fig. 4g); this effect was evident up to 8 days after drugs washout when these tumor cells are still non-proliferative. Importantly, basal H3 PTMs (K9me3 & K27me3) levels and the global changes in H3-PTMs induced by the reprogramming were NR2F1-dependent (Fig. 6d).

NR2F1 regulates residual tumor cell fate post-tumor surgery

We next studied whether NR2F1 could dictate DTC fate. After primary tumor surgery HEp3 cells form overt metastases in lungs and lymph nodes [20, 39]. In contrast, in bone marrow and spleen DTCs are detectable, but overt metastases never develop[6]. Also, at least 2 months after surgery, local recurrences develop in <17% of animals. Inducible knockdown of NR2F1 in Tet-ON-sh-NR2F1-miR-T-HEp3 cells was >60% after doxycycline (DOX) treatment (Supplementary Fig. 6c–d), without changes in its close related homologue NR2F2 levels (Supplementary Fig. 6d). Strikingly, sh-NR2F1-miR induction resulted in vigorous development of local tumor recurrences (~33% - n=15); while in mice without DOX treatment recurrences were fewer (17% n=11) and developed later (Fig. 7a). After take, sh-NR2F1-miR “ON” tumors also grew much faster than the sh-NR2F1-miR “OFF” controls reaching a much larger volume (Supplementary Fig. 6e). We also found that AzaC +atRA-induced reprogramming inhibited of tumor growth was blocked by the activation of the sh-NR2F1-miR in HEp3 cells (Fig. 7b). Thus, residual tumor cells may remain dormant and express high levels of NR2F1. Accordingly, residual solitary tumor cells (RTCs) in surgery margins showed upregulation of NR2F1 and SOX9 while the proliferation marker

P-H3 was absent (Fig. 7a). These data argue that dormant NR2F1^{hi}/SOX9^{hi}/P-H3^{lo} residual solitary tumor cells exist in surgery margins.

Importantly, when we monitored DTC burden after primary tumor surgery using human specific *Alu*-sequence qPCR, we found that by reducing NR2F1 levels (upon DOX treatment) we could increase the median number of tumor cells in spleens and lungs by 2–5 fold (Fig. 7c–d). Because this is done after primary tumor surgery and there is no more cell dissemination this result suggests that the observed increase in the number of tumor cells/organ may be due to re-awakening of dormant DTCs after NR2F1 knockdown. The detection of 0.5 to 6 x10^6 cells lung tumor cells is correlated with the presence of metastasis as reported previously at these time points[6, 39]. Interestingly, in the bone marrow where HEp3 DTCs do not proliferate, the NR2F1 knockdown caused a reduction in BM DTC burden (Fig. 7e). This may be due to NR2F1-induced survival because knockdown of this TF in the BM-HEp3 cells that express higher NR2F1 mRNA levels than the proliferative counterparts, also resulted in less dormant tumor cells recovered *in vivo* (Supplementary Fig. 6f–g).

We next tested the function of NANOG, which is downregulated upon NR2F1 depletion in BM-HEp3 cells (Supplementary Fig. 6f). To our surprise, unlike NR2F1 knockdown, NANOG knock down reactivated dormant BM-HEp3 cells *in vivo* (Supplementary Fig. 6h). It is possible that NR2F1-induced NANOG in BM-HEp3 regulates quiescence - and that NR2F1 regulates directly target genes involved in survival. Thus, depending on the organ microenvironment, NR2F1 might fulfill quiescence and/or survival functions and the former may be executed by NANOG in the BM.

Finally, we tested the link between atRA, NR2F1 and TGFβ2 signaling because we found that in the bone marrow TGFβ2 induces dormancy[6] and this cytokine mRNA was upregulated in PCa DTCs from NED vs. ADV patients. Also atRA is abundant in the BM where it regulates HSC self-renewal and differentiation[40, 41]. Treatment of T-HEp3 cells with atRA induced TGFβ2 mRNA but this was not mediated by NR2F1 (Supplementary Fig. 6i). These data support a model where microenvironmental signals propagated by retinoic acid and TGFβ2 signaling might cooperate to induce quiescence and survival of DTCs in the bone marrow.

Discussion

The role of NR2F1 in quiescence induction and cell lineage commitment [42] might explain why it is downregulated in proliferative tumors and how its re-expression by specific microenvironments or by “epigenetic therapies” induces stable dormancy in aggressive tumor cells (Fig. 8). Our findings, while limited to some extent by the use of human cancer cell lines and mouse models, still appear to provide relevant information regarding human DTC dormancy. For example, NR2F1 and TGFβ2 are more frequently upregulated in DTCs from NED than ADV PCa patients. This strongly argues that NR2F1 and TGFβ2 driven dormancy programs may be extremely long-lived in DTCs in human bone marrow (Fig. 8). Further, these prostate cancer DTCs had a significant upregulation of the whole dormancy signature identified in our dormancy model, further arguing that there may be a

commonality in the mechanisms that reprogram tumor cells into dormancy. This is also supported by our findings that the same signature predicts for longer metastasis-free periods in breast cancer patients with ER+ luminal tumors[7]. In our system of BM DTC dormancy NR2F1 drives growth arrest via SOX9 RARβ and NANOG, while NR2F1 itself favors survival while in D-HEp3 cells NR2F1 drives quiescence. How these different functions are coordinated is still unknown but it may be related to how these cells are reprogrammed into dormancy[3, 6].

The plasticity in NR2F1 expression suggests that specific signals might restore NR2F1^{high} levels in disseminated disease as observed in DTCs from PCa patients that had NED from 7–19 years. In agreement with these findings, NR2F1 expression was higher in prostate cancer patient's tumors after hormonal therapy[18]. Thus, microenvironmental signals or therapy may induce NR2F1 re-expression and determine the rate at which residual disease reactivates. A potential utility might be the detection of NR2F1, SOX9, RARβ and possibly NANOG in DTCs as biomarkers. These may pinpoint DTCs in a dormant state and with latent capacity to reactivate or that responded to epigenetic therapies[43]. These could also be tested in CTCs in M0 patients to identify precursors of dormant DTCs or re-circulating dormant tumor cells. Alternatively, as with DTCs, testing these markers on CTCs may be informative on response to therapies that activate the dormancy mechanisms.

Our data reveals something particular about NR2F1 in that in malignant cells that entered dormancy it coordinates quiescence, survival and the expression of pluripotency genes (Fig. 8). In this dormancy context NANOG may help to maintain the quiescence phase induced by NR2F1 upregulation. We cannot rule out that the pluripotency genes may allow DTCs to survive and avoid differentiation, senescence or at some point reactivate. The stability but also plasticity of the dormant phenotype was also linked to the ability of NR2F1 to induce global repressive chromatin states as evidenced by enrichment in H3K27me3 and H3K9me3 marks upon spontaneous or Aza+atRA-induced reprogramming (Fig. 8). While globally NR2F1 induces a chromatin repressive state the regulation by NR2F1 of H3K4me3 marks in its own and SOX9 and RARβ promoters indicates it can also regulate local active chromatin changes.

Specific microenvironments may contain cues (e.g. RA, TGFβ2) that in malignant tumor cells receptive to these signals may activate a dormancy program. Remarkably, NR2F1 appears to execute such a program in occult DTCs in several organs and in the surgery margins by inducing a specific combination of pluripotency (NR2F1^{high}/[NANOG/Sox2]^{high}) and quiescence (SOX9^{high}/RARβ^{high}/p27^{high}) genes. This may explain the longer metastasis-free periods in patients carrying NR2F1^{high} tumors (and putative NR2F1^{high} DTCs)[7, 18].

Our results show that "epigenetic therapies" (demethylating agents) currently used in patients[43] could induce dormancy when used at low doses and combined with atRA (Fig. 8). Remarkably, key genes (e.g. RARβ, CDKN1A) that were induced by the p38α/β [3, 7], were also induced by demethylating agents [43]. Our combination of "differentiation" and "epigenetic" therapies or the combination of specific transcription factors (e.g. NR2F1, SOX9 and RARβ) might be a strategy to generate **i**nduced **d**ormant **c**ancer **c**ells (iDCCs).

This may provide the basis for designing new therapeutics to prevent residual disease from reactivating after tumor surgery and/or chemotherapy. Such “dormancy-inducing therapies” could be used to convert residual proliferative tumor cells into dormancy and/or prevent pre-existing dormant cells from re-awakening. On the other hand, in vitro generation of iDCCs or dormant DTCs obtained from different microenvironments may allow discovering the survival mechanisms that allow them to persist over time and eradicate them. That bone marrow DTCs may require NR2F1 for survival suggests that targeting the downstream executors of the survival program, may be useful to eliminate DTCs in cancers that primarily target bone such as prostate cancer and ER+ luminal breast cancer. It also implies that a global single approach to target all disseminated cells found in different tissues in a patient may not be the best scenario. Perhaps a combination of drugs that specifically target key dormancy-regulating genes in specific microenvironments might be needed.

METHODS

Cell lines

Tumorigenic (T-HEp3) HEp3 cells were derived from a lymph node metastasis from a HNSCC patient as described previously[26] and kept as PDX (patient-derived xenografts) in CAMs. Dormant D-HEp3 cells were obtained by passing T-HEp3 cells for more than 40 generations *in vitro*[26]. Dormant (BM-HEp3) and proliferative (Lu-HEp3) cells derived from bone marrow- and lung-derived T-HEp3 DTCs were described previously[6]. When cultured in vitro all these cells were passaged in DMEM cell growth medium (Dulbeco’s modified medium with 10% of fetal bovine serum (FBS) and 100 U penicillin/0.1 mg/ml streptomycin). The 4T1 cells are derived from a single spontaneous primary mammary tumor that arose in a wild-type BALB/c mouse [44]. ShNR2F1miR cells were generated by TURBO-RFP-shNR2F1miR encoding lentivirus infection of T-HEp3 cells then selected with puromycin (2.5 μg/ml). For the MMTV-myc studies, primary cultures from MMTV-myc mouse tumors[45] were transfected with pGS5-empty or pGS5-Nr2f1. Briefly, MMTV-myc tumor cells were isolated by adding collagenase for 30 min at 37°C. Then, suspension of cells were plated in 10 cm dishes to allow for fibrosblast to attach and the resuspended cells were treated with PBS-EDTA (2mM) for 15 min at 37°C to reach single cell suspension. Finally, tumor cells were plated and grown in DMEM:F12 medium with 5% horse serum, EGF (20 ng/ml), Hydrocortisone (0.5 mg/ml), cholera toxin (100 ng/ml), insulin (10 ug/ml), penicillin/streptomycin (1x solution). pCDNA3.1(+) was used as a selection marker by co-transfection in a ratio 10:1. G418 resistant cells were selected by cloning dilution. SQ20b, MCF-7 and FaDu cells were obtained from ATCC and were grown in the same medium as T-HEp3 cells. 4T1 and PC3 were obtained from ATCC and grown in RPMI medium with 10% of FBS.

Reprogramming protocol

After seeding T-HEp3 cells were grown in DMEM high glucose media plus 10% of charcolized serum and penicillin/streptomycin and the addition of Azacytidyne (5-AzaCytidine, 5nM) for 24 hrs. Next day, fresh AzaC (5nM) was added (See supplementary Fig 4F). Then, media was changed for serum-free media plus atRA (2 μM) for 48hs. All this treatment is designed as pre-reprogramming step (pre-step). Subsequently, media was

changed for normal growing media without the addition of any drug (post-step) and with this started the post-reprogramming protocol.

Reagents and antibodies

Charcoal Stripped FBS One Shot (Gibco, Life technology, NY, USA), 5-azadeoxycytidine (Sigma, MO, USA), atRA (Sigma, MO, USA), senescence beta galactosidase kit (Cell Signaling, MA, USA), Dual luciferase reporter system (Promega, Wisconsin, USA), trizol (Invitrogen, NY, USA), NR2F1 antibody for western blot (R&D systems, MN, USA), NR2F1 antibody for IF and IHC (Abcam, MA, USA), p27, p21, and cleaved-caspase 3 (Cell signaling, MA, USA), Ki67 (Invitrogen, NY, USA), SOX9 (Millipore, MA, USA). Human NR2F1 plasmid was a kind gift from Dr. Gilles Salbert (Rennes University, France). Mouse NR2F1 plasmid was a kind gift from Dr. Lorraine Gudas (Weill Cornell Medical College). All primary antibodies for IF/IHC were used at a dilution of 1:100.

Xenograft studies

All animal studies were approved by Institutional Animal Care and Use Committees (IACUC) at Mount Sinai School of Medicine Protocol ID: 08-0366. Tumor growth on chick embryo CAMs or Balb/c nude mice has been described previously[46]. Briefly, 150 x10^3 T-HEp3 cells were inoculated on the chicken embryo chorioallantoic membrane and allowed them to grow for the indicated times in each experiment (from 4 to 7 days). Dormant D-HEp3 and BM-HEp3 cells were inoculated into CAMs at 500 x10^3 cells per egg. For atRA *in vivo* experiments, 150 x10^3 T-HEp3 cells were resuspended in 50 μl PBS in the presence of atRA (2 μM) or DMSO and inoculated into each CAM. 24 hrs. post-inoculation 50 μl of PBS plus atRA (2 μM) or DMSO were added on top of each egg. On day 4, the same treatment was repeated. Tumors were harvested at day 5, minced, digested with collagenase-1A (Sigma - C9891) for 30 min at 37°C and tumor cells, recognized by their very large diameter, were counted with a hemocytometer. For serial transplantation studies of HEp3 tumors on CAM, HEp3 tumors were minced and dissociated with collagenase-IA, tumor cells were counted and a single cell suspension (150×10^3 cells in 50μl PBS) from each tumor was reinoculated on CAMs. For RNA interference studies, transfections of cells with siRNAs targeting the desired sequences or control scrambled siRNA were performed as previously described[3]. 24h after transfection 150×10^3 cells were inoculated on the CAM of 9–10-day-old chicken embryos (Charles River). Four days post-inoculation, the number of tumor cells per nodule was counted. siRNAs knockdown were analyzed by QPCR.

For the HEp3 xenograft studies, 750 x10^3 cells were injected subcutaneously in 8 weeks-old females BALB/c nu/nu mice (Jackson Laboratories) in the interscapular region. Mice were inspected every 48hs and arising tumors were measured with calipers in two perpendicular diameters. Mice were kept (~14 days) until primary tumors developed and grew up to ~500–800 mm^3. Mice were then injected with anesthetics ketamine 80–120 mg i.p. and xylazine 5 mg i.p, and an incision of ~1cm above the base of the tumor was performed. This allows gently scoop-out the tumor tissue and leaving sufficient skin to close the wound with sutures. Sutures were done using a wound clipper. In the doxycycline-induced depletion of NR2F1 studies, mice were injected i.p. with 25mg/kg of doxycycline or vehicle every 48 hrs. For the MMTV-myc tumor studies, 1000 or 10,000 MMTV-Myc-vector or MMTV-

Myc-NR2F1 cells were orthotopically injected in the mammary fat pad of synergetic FvB mice. Tumors were detectable from day 7 and were measured every other day. Animals were sacrificed when tumors reached 500mm^3 size.

Immunohistochemistry and Immunofluorescence assays—Paraffin embedded sections from human HNSCC tumors and lymph node metastasis and breast carcinoma tissues were stained for NR2F1 expression after quenching endogenous peroxidase activity. Binding of the primary antibody was carried out at 4°C overnight, detected by anti-rabbit secondary antibody (1 hour at room temperature) and revealed using DAB Chromagen. Paraffin embedded sections from T-HEp3 and D-HEp3 tumors were stained for the followed antigens: SOX9 (dilution of Ab 1:150 for D-HEp3 and 1:75 for T-HEp3), NR2F1 (1:100 for D-HEp3 and 1:50 for T-HEp3), Ki67 (dilution of ab 1:100). For immunofluorescence assays: tumor cells seeded in coverslips were fixed with 4% paraformaldehyde (PFA) in PBS and were permeabilized with 0.1% Triton X-100. Cells were then blocked with PBS containing 3% normal goat serum (NGS).

Gene expression profiling from T- and D-HEp3 cells in vivo—GFP-tagged T-HEp3 and D-HEp3 cells were inoculated and allowed to grow (T-HEp3) or enter dormancy (D-HEp3) for one week. Then 5 T-HEp3 tumors or 5 D-HEp3 dormant nodules were processed for FACS and GFP+ cells were used to extract RNA. This RNA (10 ug) was used to perform gene expression profiling using the Affymetrix HG-U133-PLUS2 arrays. The analysis of the gene expression profiles was performed as described in[3] and the data is deposited in the Gene Expression Omnibus under the accession number GSE58588. Additional methods can be found associated with the profiles in the GEO database. The following link has been created to allow review of record GSE58588 while it remains in private status: http://www.ncbi.nlm.nih.gov/geo/query/acc.cgi?token=ovilmukmxluvpaj&acc=GSE58588

Human prostate cancer DTC isolation and expression profiling—Individual prostate cancer DTCs were isolated from the bone marrow of post-radical prostatectomy patients with no evidence of disease (NED – dormant disease) or advanced proliferative disease (ADV)[31]. Samples were obtained from patients who signed written informed consent. The study was approved by the Cancer Consortium institutional review board at the Fred Hutchinson Cancer Research Center and the University of Washington (Protocol #7350). NED patients showed undetectable PSA level (<0.1ng/mL) 7–18 years after prostatectomy. ADV patients showed disease progression with failed treatment or existing distant metastasis. Seven individual NED cells (4 patients) and 37 ADV cells (6 patients) were amplified using the WT-OviationTM one-direct system (NuGEN) and single-cell gene expression was analyzed by Agilent 4×44K Human Microarrays. The analysis of the gene expression profiles of single cells obtained from patients with advanced disease and patients with no evidence of disease was performed on the profiles in Gene Expression Omnibus database under the accession number GSE48995. All isolation methods and procedures are described therein. The following link has been created to allow review of record GSE48995 while it remains in private status: http://www.ncbi.nlm.nih.gov/geo/query/acc.cgi?token=ndclzsckieyygte&acc=GSE48995

Senescence assays—Tumors were harvested, digested with collagenase-1A (Sigma - C9891) for 30 min at 37°C and then the manufacturer's protocol for senescence detection (Cell Signaling, # 9860S) was followed.

RNA interference

Transfections of siRNAs targeting the desired sequences or scrambled siRNA, were performed using siPORT NeoFX (Ambion). Detached cells were resuspended and overlaid onto the transfection complexes. After 24h under normal cell culture conditions, cells were either used for *in vivo* experiments or lysed for Immunoblotting and/or qPCR. Human siNR2F1 sequence sense: CUCUCAUCCGCGAUAUGUU; antisense: AACAUAUCGCGGAUGAGAG (SIGMA, SASI_Hs01_00095428/AS). Human siNANOG sequence sense: GUGUGUACUCAAUGAUAGA, antisense: UCUAUCAUUGAGUACACAC (SIGMA, SASI_Hs01_00163355/AS). Human siSOX9 sequence sense: CGUGUGAUCAGUGUGCUAA; antisense:UUAGCACACUGAUCACACG (SIGMA, SASI_Hs01_00240733/AS). Human siRARβ sequence sense: CAUUGCUGGAAGCACUAAA; antisense: UUUAGUGCUUCCAGCAAUG (SIGMA, SASI_Hs01_00237846/AS).

Immunoblotting, RT-PCR and quantitative qPCR—Images for Immunoblotting have been cropped for presentation. Full size images are presented in supplementary figures 7–11. RT-PCR and quantitative qPCR were performed as described previously [3]. NR2F1 human forward primer: GCCTCAAAGCCATCGTGCTG, NR2F1 human reverse primer: CCTCACGTACTCCTCCAGTG, SOX9 human forward primer: CACTCCTCCTCCGGCATG, SOX9 human reverse primer: GGCTGCACGTCGGTTTTGG, RARβ human forward primer: GTACCACTATGGGGTCAGCG, RARβ human reverse primer: CGACAGTATTGGCATCGATTCC, NANOG human forward primer: CTAAGAGGTGGCAGAAAAACA, NANOG human reverse primer: CTGGTGGTAGGAAGAGTAAAGG, SOX2 human forward primer: GTTGTCAAGGCAGAGAAGAG, SOX2 human reverse primer: GAGAGAGGCAAACTGGAATC, TUBULIN human forward primer: CCCTCCAAGCTCTACTCT, TUBULIN human reverse primer: GACCAAGGCTGGTCTCTTTC, HES-1 human forward primer: CCCAGCCAGTGTCAACACGACA, HES-1 human reverse primer: GGTACCGCCCTTACCTTTCTGTGC, p27 human forward primer: GGTTAGCGGAGCAATGCGCA, p27human reverse primer: AACCGGCATTTGGGGAACCGTC, p15 human forward primer: TGGGGTGGGAAAGTGGATTGCA, p15 human reverse primer: CCCAGTGCAGAGGTGTTCAGGTCT, p16 human forward primer: GCTGCTCACCTCTGGTGCCAAA, p16 human reverse primer: ACCTGCGCACCATGTTCTCG

Detection of DTCs via *Alu*-qPCR

Human cells within mouse BM, lungs and spleen were detected by real-time *Alu* qPCR, essentially as described [47]. Briefly, BM flushes were snap frozen in liquid nitrogen and the

genomic DNA was extracted using the Extract-N-Amp kit from Sigma (XNAT2-1KT). 30ng of genomic DNA was used per PCR reaction. Amplification of mice *GAPDH* was used as an internal control for the total amount of tissue. The ratio between *hAlu* and *mGAPDH* is used for comparative purposes between experimental groups. The primers for *hAlu* sequences and mice *GAPDH* were: *hAlu* sense (ACGCCTGTAATCCCAGCACTT) and *hAlu* antisense (TCGCCCAGGCTGGGTGCA), *mGAPDH* FW (ATGGTGAAGGTCGGTGTGA), *mGAPDH* RV (CGTTGATGGCAACAATCTC). Each assay included 2 negative controls (water and genomic DNA extracted from BM, lung and spleen from a mouse that has not been injected with human cells), a positive control (human genomic DNA), and the experimental samples in triplicate. The actual number of tumor cells present in each tissue sample was determined using a standard curve generated by serial dilution of HEp3 cells. Briefly, organ specific cells were collected from nude mice that did not bear tumors. HEp3 cells were serially diluted into mice organ specific single cell suspensions and the genomic DNA was extracted and amplified. The actual number of tumor cells could be determined over a range of 10–1000 cells/BM, 100–10000 cells/spleen and over 100–1000000 cells/lung.

Sphere-forming assay

After the pre-reprogramming protocol T-HEp3 cells were seeded in low-attachment 6-multi-well plates (100 x10^3 cells/well) in stem cell media (DMEM:F12, B27 supplement, EGF). Sphere formation was observed by light microscope and spheres were counted at day 6. MMTV-myc cells: MMTV-myc control cells or MMTV-myc Nr2f1 cells were trypsinized, dissociated by pipetting and filtering through a 40 μm pore cell strainer. 1×10^5 cells per condition were plated by triplicates in ultra low adhesion 6-well plates (Corning, Corning, NY, USA) and incubated in serum-free F12/DMEM 50:50 medium (Cellgro, Mediatech, Inc., Manassas, VA, USA) supplemented with 20 ng/ml EGF and 1:50 B27 Supplement (Invitrogen, Carlsbad, CA, USA).

Flow Cytometry

For the characterization of the progenitor containing compartments, each well was dissociated with PBS-EDTA at 37°C with gentle shaking, filtered through a 40 μm cell strainer and incubated with PE or APC-conjugated anti-CD24 Ab (BD Pharmingen, San Jose, CA, USA), APC-conjugated anti-CD29 Ab (Invitrogen, Camarillo, CA, USA).

Sequenom array

The bisulfite PCR primers for the Sequenom array were designed using EpiTYPER software (Supplementary Table III). Genomic DNA from each sample was prepared using QIAamp DNA mini kit (Qiagen) and the concentration and quality were determined by measuring the absorbance at 260 nm and 280 nm in a spectrophotometer (NanoDrop 8000, Thermo Scientific). DNA was subjected to bisulfite modification by using the EZ DNA Methylation kit (Zymo Research). Purified DNA samples were forwarded to Sequenom MassARRAY core facility at Cornell University Institute of Biothechnology.

Chromatin immunoprecipitation (ChIP)

ChIP was performed as previously described and followed by qPCR analysis[48]. The antibodies used for the immunoprecipitation were the following: H3K4me3 (ab1012, Abcam), H3K9me3 (ab8898, Abcam) and H3K27ac (ab4729, Abcam). Real-time PCR reactions (Roche) were performed in triplicates using primers for the correspondent genomic regions. Fold enrichment over 1% input was calculated using the 2DeltaCt method. Primers for ChiP are described in Supplementary Table IV.

Statistical analysis

For DTCs detection experiments the p-values were estimated using Mann-Whitney non-parametric test with one-tailed *p* values ≤0.05 considered significant. For all the rest experiments unpaired t test were used with a 95% confidence. For *in vitro* experiments a minimum of triplicates per group and repetition of at least 3 times was applied to achieve reproducibility. For *in vivo* experiments a minimum of 5 tumors for CAM assays and a minimum of 8 mice was assessed to achieve reproducibility.

Supplementary Material

Refer to Web version on PubMed Central for supplementary material.

Acknowledgments

We thank the Bernstein, Farias and Aguirre-Ghiso labs as well as Peter Nelson, Robert L Vessella and Lynda Snyder for useful discussions. Grant Support: Samuel Waxman Cancer Research Foundation Tumor Dormancy Program to J.A.A-G. E.F.F and E.B., NIH/National Cancer Institute (CA109182, CA163131), NIEHS (ES017146) and NYSTEM to J.A.A-G, Hirschl/Weill-Caulier Trust Research Award to E.B., DoD-BCRP Grant BC100975 to A.G.M. and DoD-BCRP Grant BC112380 to M.S.S. NIH RC1 CA144825-0 ARRA Challenge, Janssen Research and Development LLC to Peter S Nelson, Robert L. Vessella, and Linda Snyder.

References

1. Sosa MS, Avivar-Valderas A, Bragado P, Wen HC, Aguirre-Ghiso JA. ERK1/2 and p38alpha/beta signaling in tumor cell quiescence: opportunities to control dormant residual disease. Clin Cancer Res. 2011; 17:5850–5857. [PubMed: 21673068]
2. Sosa MS, Bragado P, Aguirre-Ghiso JA. Mechanisms of disseminated cancer cell dormancy: an awakening field. Nature reviews Cancer. 2014; 14:611–622. [PubMed: 25118602]
3. Adam AP, et al. Computational identification of a p38SAPK-regulated transcription factor network required for tumor cell quiescence. Cancer Res. 2009; 69:5664–5672. [PubMed: 19584293]
4. Onder TT, et al. Chromatin-modifying enzymes as modulators of reprogramming. Nature. 2012; 483:598–602. [PubMed: 22388813]
5. Marion RM, et al. A p53-mediated DNA damage response limits reprogramming to ensure iPS cell genomic integrity. Nature. 2009; 460:1149–1153. [PubMed: 19668189]
6. Bragado P, et al. TGF-beta2 dictates disseminated tumour cell fate in target organs through TGF-beta-RIII and p38alpha/beta signalling. Nat Cell Biol. 2013; 15:1351–1361. [PubMed: 24161934]
7. Kim RS, et al. Dormancy signatures and metastasis in estrogen receptor positive and negative breast cancer. PloS one. 2012; 7:e35569. [PubMed: 22530051]
8. Qiu Y, et al. Spatiotemporal expression patterns of chicken ovalbumin upstream promoter-transcription factors in the developing mouse central nervous system: evidence for a role in segmental patterning of the diencephalon. Proc Natl Acad Sci U S A. 1994; 91:4451–4455. [PubMed: 8183930]

9. Zhuang Y, Gudas LJ. Overexpression of COUP-TF1 in murine embryonic stem cells reduces retinoic acid-associated growth arrest and increases extraembryonic endoderm gene expression. Differentiation; research in biological diversity. 2008; 76:760–771.
10. Rada-Iglesias A, et al. Epigenomic annotation of enhancers predicts transcriptional regulators of human neural crest. Cell Stem Cell. 2012; 11:633–648. [PubMed: 22981823]
11. Fackler MJ, et al. Quantitative multiplex methylation-specific PCR assay for the detection of promoter hypermethylation in multiple genes in breast cancer. Cancer Res. 2004; 64:4442–4452. [PubMed: 15231653]
12. Ginos MA, et al. Identification of a gene expression signature associated with recurrent disease in squamous cell carcinoma of the head and neck. Cancer Res. 2004; 64:55–63. [PubMed: 14729608]
13. Richardson AL, et al. X chromosomal abnormalities in basal-like human breast cancer. Cancer Cell. 2006; 9:121–132. [PubMed: 16473279]
14. Hou J, et al. Expression profiling-based subtyping identifies novel non-small cell lung cancer subgroups and implicates putative resistance to pemetrexed therapy. J Thorac Oncol. 7:105–114. [PubMed: 22134068]
15. Grasso CS, et al. The mutational landscape of lethal castration-resistant prostate cancer. Nature. 2012; 487:239–243. [PubMed: 22722839]
16. Taylor BS, et al. Integrative genomic profiling of human prostate cancer. Cancer Cell. 2010; 18:11–22. [PubMed: 20579941]
17. Smits BM, et al. The gene desert mammary carcinoma susceptibility locus Mcs1a regulates Nr2f1 modifying mammary epithelial cell differentiation and proliferation. PLoS genetics. 2013; 9:e1003549. [PubMed: 23785296]
18. Thompson VC, et al. A gene signature identified using a mouse model of androgen receptor-dependent prostate cancer predicts biochemical relapse in human disease. Int J Cancer. 2011
19. Kim J, et al. A Myc network accounts for similarities between embryonic stem and cancer cell transcription programs. Cell. 2010; 143:313–324. [PubMed: 20946988]
20. Aguirre-Ghiso JA, Ossowski L, Rosenbaum SK. Green fluorescent protein tagging of extracellular signal-regulated kinase and p38 pathways reveals novel dynamics of pathway activation during primary and metastatic growth. Cancer Res. 2004; 64:7336–7345. [PubMed: 15492254]
21. Aguirre-Ghiso JA, Estrada Y, Liu D, Ossowski L. ERK(MAPK) activity as a determinant of tumor growth and dormancy; regulation by p38(SAPK). Cancer Res. 2003; 63:1684–1695. [PubMed: 12670923]
22. Aguirre-Ghiso JA, Liu D, Mignatti A, Kovalski K, Ossowski L. Urokinase receptor and fibronectin regulate the ERK(MAPK) to p38(MAPK) activity ratios that determine carcinoma cell proliferation or dormancy in vivo. Molecular biology of the cell. 2001; 12:863–879. [PubMed: 11294892]
23. Schewe DM, Aguirre-Ghiso JA. ATF6alpha-Rheb-mTOR signaling promotes survival of dormant tumor cells in vivo. Proc Natl Acad Sci U S A. 2008; 105:10519–10524. [PubMed: 18650380]
24. Liu D, Aguirre Ghiso J, Estrada Y, Ossowski L. EGFR is a transducer of the urokinase receptor initiated signal that is required for in vivo growth of a human carcinoma. Cancer Cell. 2002; 1:445–457. [PubMed: 12124174]
25. Aguirre Ghiso JA. Inhibition of FAK signaling activated by urokinase receptor induces dormancy in human carcinoma cells in vivo. Oncogene. 2002; 21:2513–2524. [PubMed: 11971186]
26. Ossowski L, Reich E. Changes in malignant phenotype of a human carcinoma conditioned by growth environment. Cell. 1983; 33:323–333. [PubMed: 6407756]
27. Huang S, et al. ZNF423 is critically required for retinoic acid-induced differentiation and is a marker of neuroblastoma outcome. Cancer Cell. 2009; 15:328–340. [PubMed: 19345331]
28. Bragado P, et al. Analysis of marker-defined HNSCC subpopulations reveals a dynamic regulation of tumor initiating properties. PloS one. 2012; 7:e29974. [PubMed: 22276135]
29. Florenes VA, et al. TGF-beta mediated G1 arrest in a human melanoma cell line lacking p15INK4B: evidence for cooperation between p21Cip1/WAF1 and p27Kip1. Oncogene. 1996; 13:2447–2457. [PubMed: 8957087]
30. Sang L, Coller HA, Roberts JM. Control of the reversibility of cellular quiescence by the transcriptional repressor HES1. Science. 2008; 321:1095–1100. [PubMed: 18719287]

31. Chery L, et al. Characterization of single disseminated prostate cancer cells reveals tumor cell heterogeneity and identifies dormancy associated pathways. Oncotarget. 2014; 5:9939–9951. [PubMed: 25301725]
32. Husemann Y, et al. Systemic spread is an early step in breast cancer. Cancer Cell. 2008; 13:58–68. [PubMed: 18167340]
33. Lu X, et al. Predicting features of breast cancer with gene expression patterns. Breast cancer research and treatment. 2008; 108:191–201. [PubMed: 18297396]
34. Curtis C, et al. The genomic and transcriptomic architecture of 2,000 breast tumours reveals novel subgroups. Nature. 2012; 486:346–352. [PubMed: 22522925]
35. Lin B, et al. Orphan receptor COUP-TF is required for induction of retinoic acid receptor beta, growth inhibition, and apoptosis by retinoic acid in cancer cells. Molecular and cellular biology. 2000; 20:957–970. [PubMed: 10629053]
36. Afonja O, et al. RAR agonists stimulate SOX9 gene expression in breast cancer cell lines: evidence for a role in retinoid-mediated growth inhibition. Oncogene. 2002; 21:7850–7860. [PubMed: 12420222]
37. Drivdahl R, et al. Suppression of growth and tumorigenicity in the prostate tumor cell line M12 by overexpression of the transcription factor SOX9. Oncogene. 2004; 23:4584–4593. [PubMed: 15077158]
38. Qiu Y, Krishnan V, Pereira FA, Tsai SY, Tsai MJ. Chicken ovalbumin upstream promoter-transcription factors and their regulation. The Journal of steroid biochemistry and molecular biology. 1996; 56:81–85. [PubMed: 8603050]
39. Ossowski L, Russo H, Gartner M, Wilson EL. Growth of a human carcinoma (HEp3) in nude mice: rapid and efficient metastasis. Journal of cellular physiology. 1987; 133:288–296. [PubMed: 3119604]
40. Ghiaur G, et al. Regulation of human hematopoietic stem cell self-renewal by the microenvironment's control of retinoic acid signaling. Proc Natl Acad Sci U S A. 2013; 110:16121–16126. [PubMed: 24043786]
41. Purton LE, et al. RARgamma is critical for maintaining a balance between hematopoietic stem cell self-renewal and differentiation. The Journal of experimental medicine. 2006; 203:1283–1293. [PubMed: 16682494]
42. Naka H, Nakamura S, Shimazaki T, Okano H. Requirement for COUP-TFI and II in the temporal specification of neural stem cells in CNS development. Nat Neurosci. 2008; 11:1014–1023. [PubMed: 19160499]
43. Tsai HC, et al. Transient low doses of DNA-demethylating agents exert durable antitumor effects on hematological and epithelial tumor cells. Cancer Cell. 21:430–446. [PubMed: 22439938]
44. Aslakson CJ, Miller FR. Selective events in the metastatic process defined by analysis of the sequential dissemination of subpopulations of a mouse mammary tumor. Cancer Res. 1992; 52:1399–1405. [PubMed: 1540948]
45. Bosch A, et al. Reversal by RARalpha agonist Am580 of c-Myc-induced imbalance in RARalpha/RARgamma expression during MMTV-Myc tumorigenesis. Breast cancer research : BCR. 2012; 14:R121. [PubMed: 22920668]
46. Aguirre Ghiso JA, Kovalski K, Ossowski L. Tumor dormancy induced by downregulation of urokinase receptor in human carcinoma involves integrin and MAPK signaling. J Cell Biol. 1999; 147:89–104. [PubMed: 10508858]
47. Zijlstra A, et al. A quantitative analysis of rate-limiting steps in the metastatic cascade using human-specific real-time polymerase chain reaction. Cancer Res. 2002; 62:7083–7092. [PubMed: 12460930]
48. Gaspar-Maia A, et al. MacroH2A histone variants act as a barrier upon reprogramming towards pluripotency. Nat Commun. 4:1565. [PubMed: 23463008]

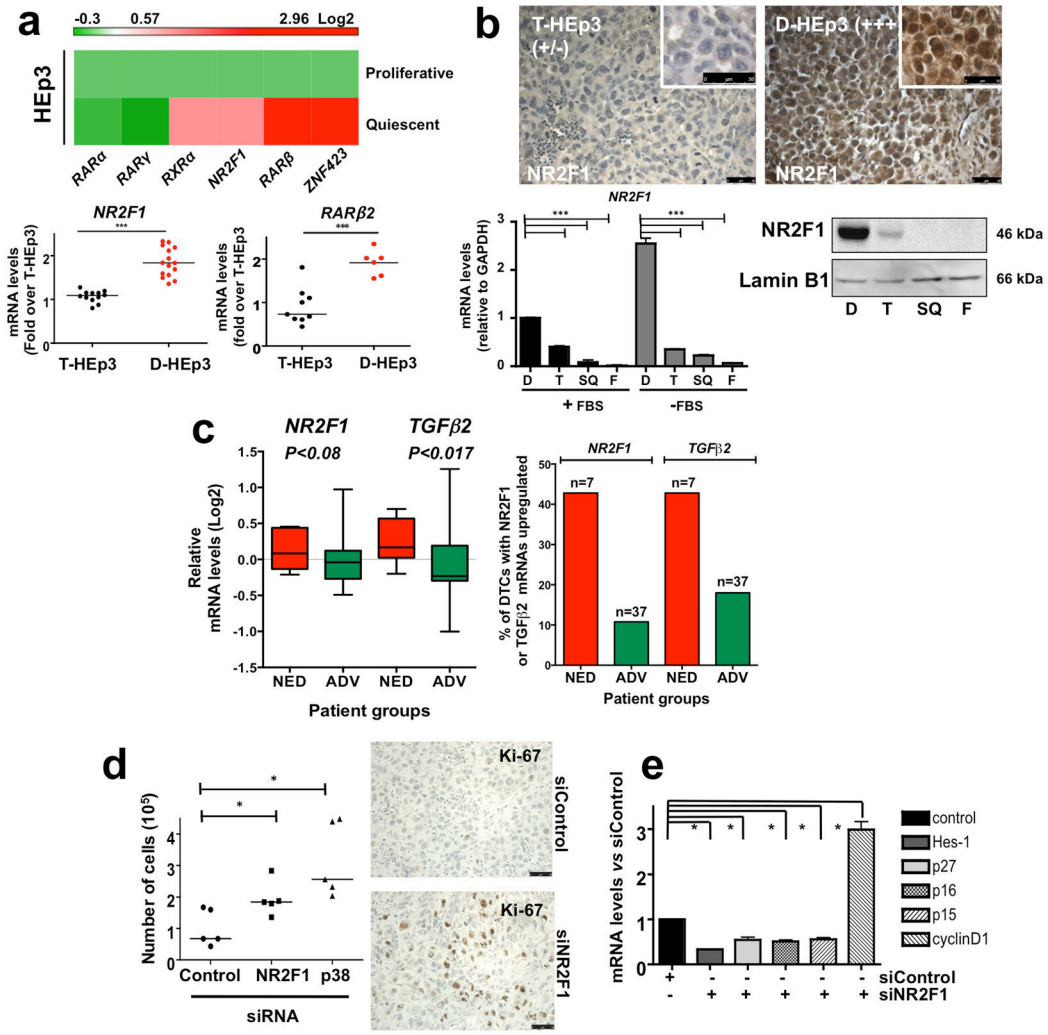

Figure 1. a) NR2F1 and RA responsive genes in quiescent HEp3 cells

Upper panel: RNA from sorted GFP-positive T-HEp3 (proliferative) and D-HEp3 (quiescent) cells grown in CAMs for 7 days was expression profiled using the Affymetrix platform. The heat map shows the Log_2-fold mRNA level change normalized to the levels in proliferative HEp3 cells. Tumors (n=5) were collected and RNA pooled and run in triplicate Affymetrix HG-U133-PLUS2 arrays. Lower panel: QPCR for NR2F1 (T-HEp3 tumors n=12, D-HEp3 tumors n=15) and RARβ2 (T-HEp3 tumors n=9, D-HEp3 tumors n=6) mRNA in T- and D-HEp3 cells grown in CAMs for 7 day. **b) IHC for NR2F1.** Upper panels, T-HEp3 tumors and D-HEp3 nodules sectioned and stained by IHC against NR2F1. Insets = higher magnification of replicate T- or D-HEp3 tumors. Bars = 50 um. Lower left panel: QPCR for NR2F1 mRNA in D= D-HEp3, T= T-HEp3, SQ= SQ20B, F= FaDu cells in the presence or absence of 10% FBS. n=3 RNA replicates/condition. Lower right panel: Nuclear fraction lysates of the indicated cell lines IB for NR2F1. LaminB1 = loading control. 3 independent experiments. Bars = 50 μm**. c) Single-cell expression profiling on bone marrow DTCs.** Left panel: BM DTCS were isolated from patients with No Evidence of Disease (NED, n=4 patients) and patient with advanced disease (ADV, n=6 patients).

Single-cell gene expressions were analyzed by Agilent 4×44K Human Microarrays and NR2F1 and TGFβ2 mRNA levels were compared between both groups. Right panel: Percentage of DTCs with high levels of NR2F1 mRNA levels were plotted for NED patients or ADV patients. n= number of DTCs. p values were obtained by Mann-Whitney test. **d) NR2F1 function in D-HEp3 cell dormancy.** Left panel: Control, NR2F1- or p38α-depleted D-HEp3 cells were inoculated into CAMs and 4 days later the total tumor cells were counted. Right panel: IHC for Ki67 in siControl or siNR2F1 tumor sections. n=5 tumors/group. **e)** QPCR for HES1, p27, p16, p15 and cyclinD1 genes from siControl or siNR2F1 tumor RNA samples. Unless stated all data are representative of at least triplicate independent experiments, n=3 RNA replicates/condition unpaired t test, *$p<0.05$, ***$p<0.0005$, SD shown. Mann-Whitney test was used for *in vivo* experiments.

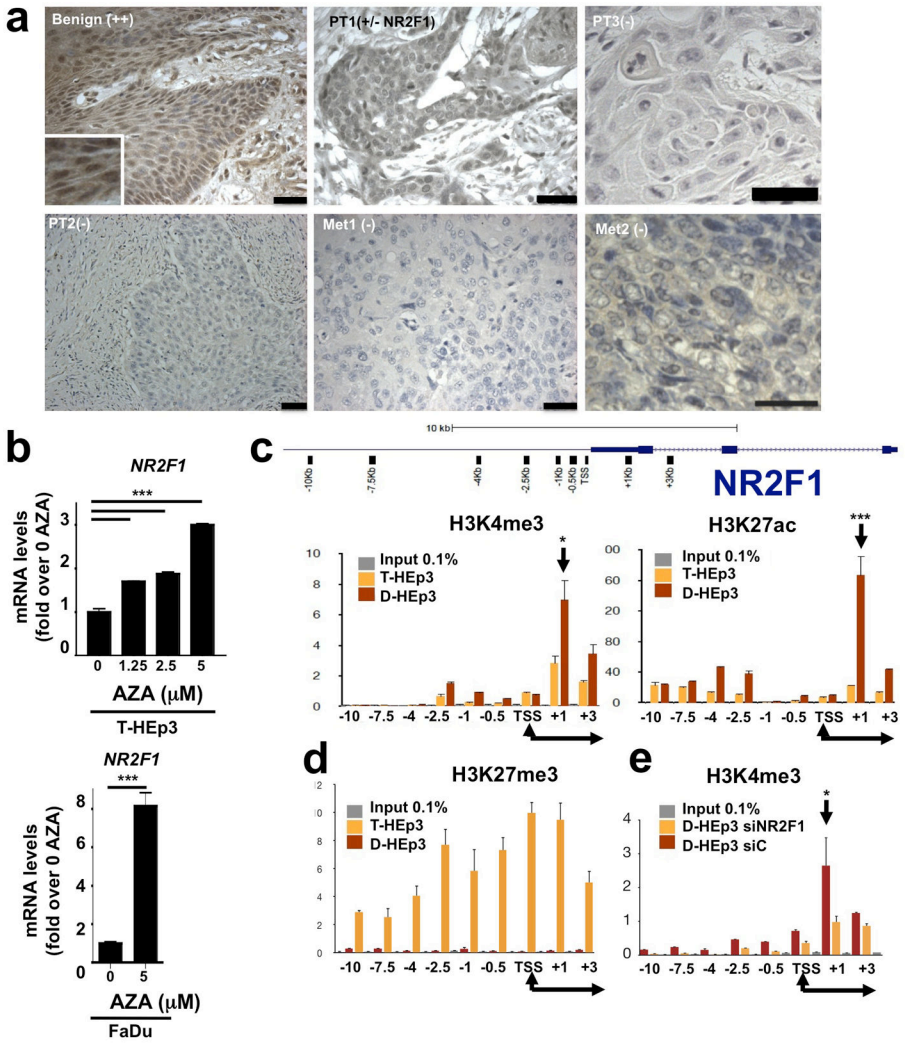

Figure 2. NR2F1 expression in HNSCC tumors and epigenetic regulation

a) NR2F1 protein detection in benign adjacent oral mucosa (Inset= magnification of NR2F1+ epithelium), in primary tumors (PT) and lymph node metastasis (met). Bars = 50 μm. Images shown are representative of n= 6 benign adjacent tissue, 15 primary tumors, 9 recurrences and 11 metastasis. **b) Azacytidine treatment and NR2F1 expression in HNSCC cells.** T-HEp3 (top panel) and FaDu (lower panel) cells were treated with 5-azacytidine (AZA) at the indicated concentrations for 2 days and NR2F1 mRNA quantified by QPCR. Y axis= AZA conditions over no AZA. ***=p<0.0005, unpaired t test. n=3 RNA samples/condition. **c–d) H3PTMs at the NR2F1 locus in T- and D-HEp3 cells.** T- and D-HEp3 cells were cultured *in vitro* followed by ChIP-qPCR analysis of the NR2F1 genomic locus for H3K4me3, H3K27ac **(c)** and H3K27me3 **(d)** histone modifications. Top scheme shows the primers used around the transcription start site (TSS) of the NR2F1 genomic locus. Bar graphs indicate fold enrichment over Input (1%), *p<0.05, **p<0.005, unpaired t test, mean ± s.d. (n=3). Arrows show sites with significant changes for the indicated histone modification in two independent experiments. All other data are representative of at least triplicate independent experiments. **e) ChIP-qPCR for H3k4me3 at the NR2F1 locus in**

D-HEp3 cells. After NR2F1 ablation (by siRNA, 50 nM) cultured cells were subjected to ChIP-qPCR for H3K4me3 at NR2F1 locus. Arrows show sites with significant changes for the indicated histone modification in two independent experiments. *$p<0.05$, unpaired t test, mean ± SD (n=3). All other data are representative of at least triplicate independent experiments, SD shown.

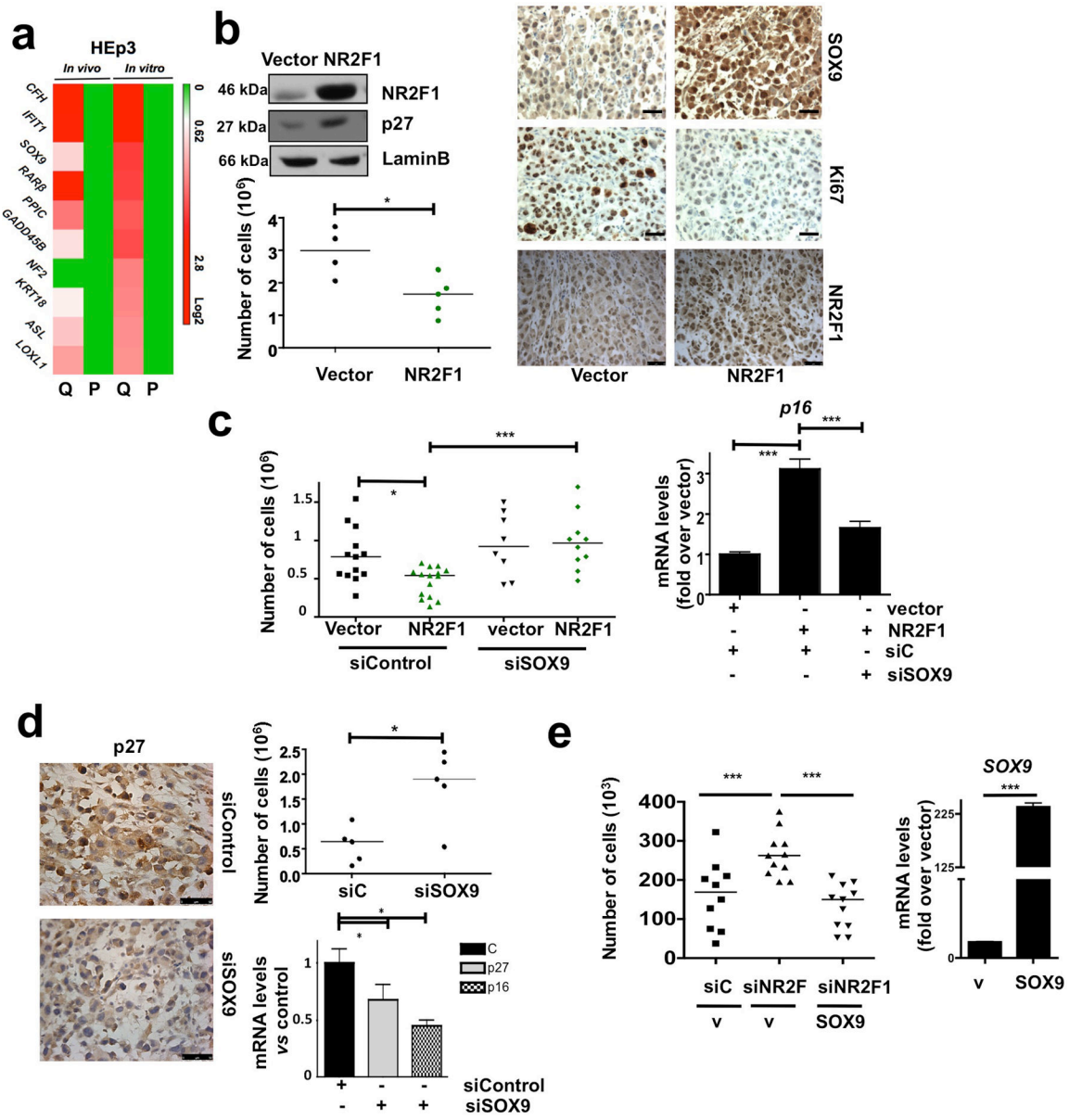

Figure 3. a) Identification of NR2F1 and RARβ targets

Heat map for the 10 genes that share NR2F1 and RARβ binding elements. Log2 gene expression changes, green= basal expression in Proliferative (P) T-HEp3 cells and increasing red intensity indicates upregulation in quiescent (Q) D-HEp3 cells. **b) Overexpression of NRF21 inhibits tumor growth.** NR2F1, p27 and Lamin-B detection in T-HEp3 cells transfected with NR2F1 or Control plasmids (top left panels) or tested for tumor growth on CAMs for 5 days (bottom left panel). n=4 tumors/group. IHC on vector or NR2F1-overexpressing tumor sections for the indicated antigens (right panels). Scale bars: 50 μm. **c) NR2F1 inhibits tumor growth *via* SOX9.** Left panel: T-HEp3 cells transfected with SOX9 or control siRNAs (50 nM) were re-transfected with empty or NR2F1 cDNA vectors. Tumor growth was quantified 4 days later on CAMs; 3 independent experiments

(left panel). Vector, n=13 tumors; siC NR2F1, n=15 tumors; siSOX9 vector, n= 8 tumors; siSOX9 NR2F1, n=10 tumors. Right panel: p16 mRNA levels relative to tubulin in T-HEp3 cells in the indicated groups. **d) SOX9 RNAi promotes D-HEp3 cell proliferation.** D-HEp3 cells were transfected with siRNA for SOX9 or control (siC, 50 nM). Left: Tumor sections from siControl and siSOX9 groups stained for p27 by IHC. Top right: growth of siControl or siSOX9-treated D-HEp3 cells on CAMs for 4 days. Bottom right: mRNA levels for p27 and p16 after 4 days *in vivo*. n= 5 tumors/group. Scale bars: 50 μm. **e) SOX9 overexpression blocks dormancy reactivation after NR2F1 RNAi.** Left panel: D-HEp3 cells were transfected with NR2F1 or control siRNAs (50 nM) and then transfected with SOX9 cDNA or empty vector. Growth of these groups was assessed on CAMs for 4 days. 2 independent experiments. Right panel: D-HEp3 cells were transfected with SOX9 cDNA or empty vector. SOX9 mRNA levels were measured by QPCR. siC vector n=10 tumors; siNR2F1 vector, n=11 tumors; siNR2F1 SOX9 n= 11 tumors. Unless stated all data are representative of at least triplicate independent experiments, n=3 RNA replicates/condition unpaired t test, *$p<0.05$, ***$p<0.0005$, SD shown. Mann-Whitney test was used for *in vivo* experiments.

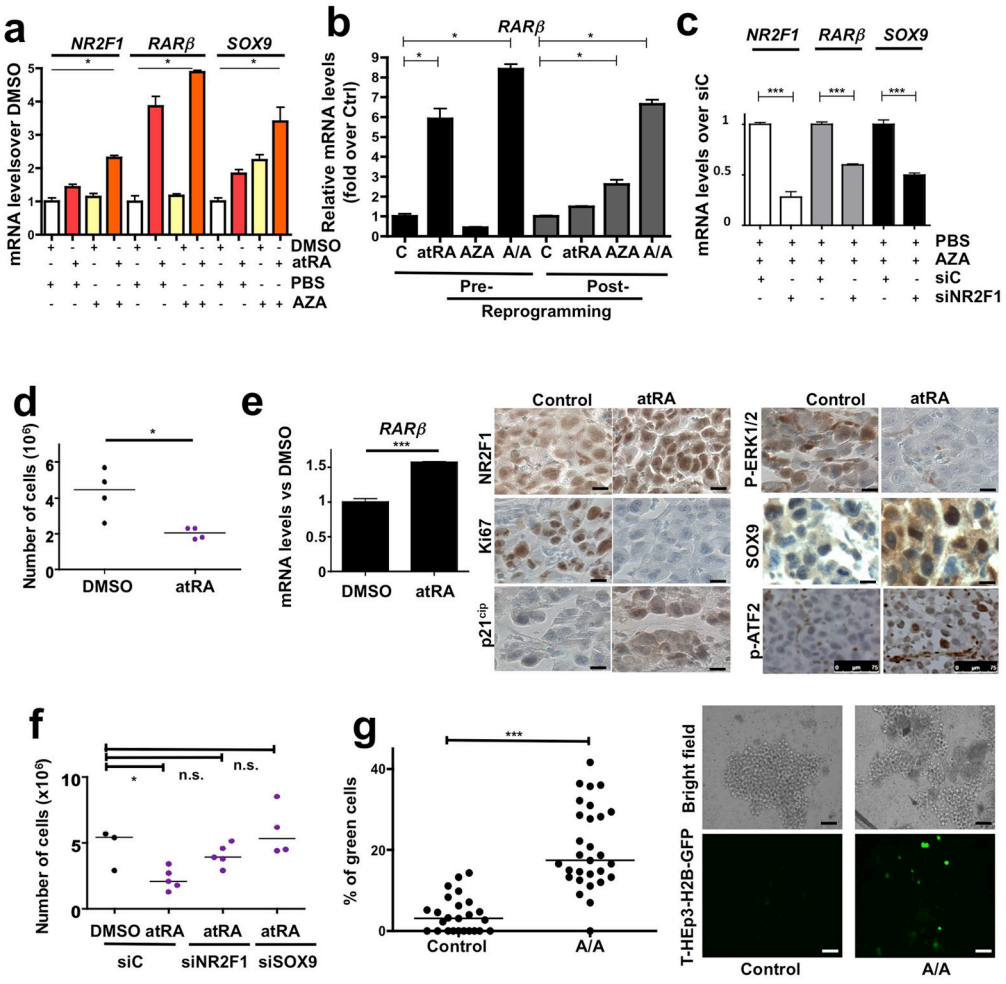

Figure 4. AzaC+atRA and NR2F1-induced reprogramming

a) T-HEp3 cells treated with 5 nM of AzaC or PBS for 48 hrs. in media + charcolized serum were washed and stimulated with atRA (2 μM) or DMSO for 48hs in serum-free media. NR2F1, RARβ and SOX9 mRNA levels measured by QPCR. *p<0.05. **b)** T-HEp3 cells were treated as in (a). Then, cells were grown in DMEM 10% FBS for 3 days without drugs and RARβ mRNA levels measured by QPCR. Pre-reprogramming=4 days of Aza+atRA treatment (see Supplementary Fig. 4f); post-reprogramming= 3 days after Aza+atRA treatment. *p<0.05 **c)** NR2F1, RARβ and SOX9 mRNA levels in T-HEp3 cells transfected with siControl or siNR2F1 (50 nM) treated as in (a) and left untreated for 3 days. *p<0.05. **d)** T-HEp3 cells were stimulated with atRA (2μM) or DMSO inoculated on CAMs (150×10^3/animal), and tumor growth scored at day 4. n=4, *p<0.05. **e)** Sections from tumors treated as in (d) were probed for RARβ mRNA levels or stained for the indicated antigens. ***p<0.0005. Scale bars:15 and 75 μm. **f)** T-HEp3 cells transfected with siRNAs for NR2F1, SOX9 or control were stimulated with atRA (2μM) or DMSO and then inoculated into CAMs (1.5×10^5 cells/embryo) as in (d). *p<0.05. siC DMSO group, n=3 tumors; siC atRA group, n=5 tumors; siNR2F1 atRA group, n=5 tumors; siSOX9 atRA group, n=4 tumors. **g)** Quantification (left) of H2B-GFP label retaining T-HEp3 cells *in vivo* after

treatment as in (a) except that 3 days before the treatment cells were induced with doxycycline to induce H2B-GFP; ***p<0.0001. Right: phase contrast (top) and GFP channel (bottom) images of H2B-GFP tumor explants after gentle mechanical mincing. Unless stated all data are representative of at least triplicate independent experiments. y=percentage of positive green cells in 4 fields. n=6 tumors per group. Scale bars: 45 μm. Unless stated all data are representative of at least triplicate independent experiments, n=3 RNA replicates/condition unpaired t test, SD shown. Mann-Whitney test was used for *in vivo* experiments.

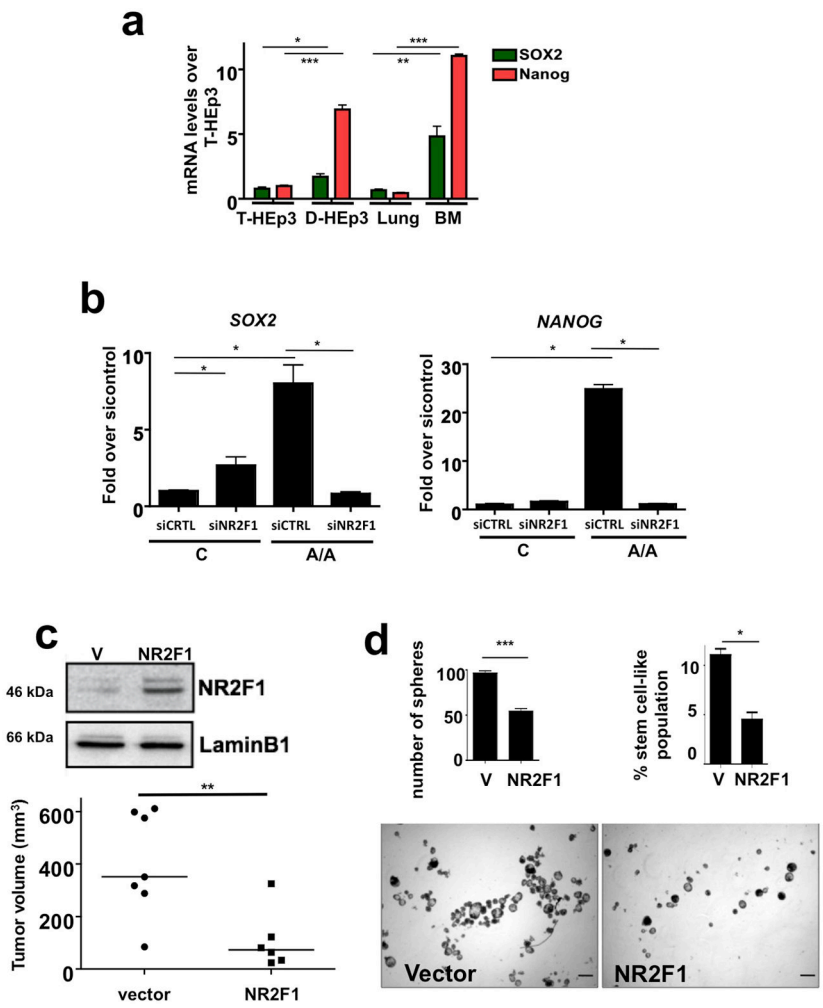

Figure 5. NR2F1 and tumor initiating properties

a) Expression of SOX2 and NANOG in proliferative vs. dormant HEp3 sublines. Cells were grown in complete medium and RNA was extracted and converted to cDNA. SOX2 and NANOG mRNA levels were measured by QPCR. ***p<0.0005, *p<0.05, **p<0.005, unpaired t test. Lung: a line derived from HEp3 lung DTCs (proliferative). BM: a line derived from HEp3 BM DTCs (dormant). **b) AzaC+atRA treatment requires NR2F1 to induce SOX2 and NANOG.** T-HEp3 cells treated with AzaC+atRA or PBS/DMSO were transfected with siControl or siNR2F1 and SOX2 and NANOG mRNAs were detected by QPCR. **c) NR2F1 inhibits MMTV-Myc tumorsphere formation capacity.** MMTV-myc cells stably expressing a control or murine NR2F1 cDNA were inoculated orthotopically in syngeneic FvB mouse (1000 cells/mouse). Tumor size was measured daily and the final tumor size is shown. In all panels experiments were performed a minimum of two times. V=vector, *p<0.05, unpaired t test. N=6 per condition, y=tumor volume. **d)** Same cells as c) were cultured in mammospheres conditions and quantified (top left) and 8 days later cells were analyzed by FACS for CD29 and CD24 markers (top right), quantified and imaged (bottom left and right). Pictures show MMTV-myc mammoespheres. V=vector, ***p<0.0005, unpaired t test. n=3 wells per condition, y=number of spheres per conditions.

Scale bars= 200 μm. Unless stated all data are representative of at least triplicate independent experiments and QPCR: n=3 RNA replicates/condition, SD shown. Mann-Whitney test was used for *in vivo* experiments.

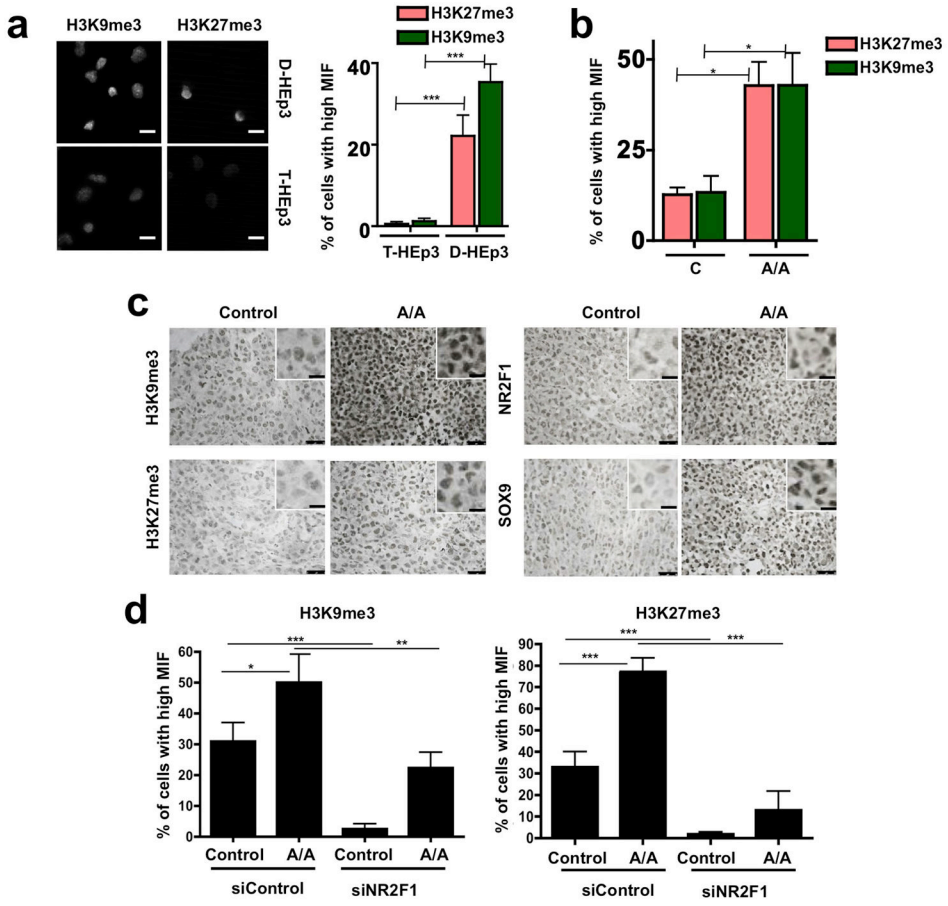

Figure 6. NR2F1 and global H3-PTMs

a) H3K27me3 and H3K9me3 levels in T- and D-HEp3 cells. D-HEp3 and T-HEp3 cells grown on coverslips were fixed with 4% PFA and stained with anti-H3K27me3 and -H3K9me3 antibodies (left panels); representative images are shown. Quantification (right panel) was performed after setting up fixed arbitrary units of immunoflourescence intensity. High mean intensity (MIF) fluorescence was scored using Metamorph for each group. ***p<0.0005, unpaired t test. Scale bars: 40 μm. **b) Effect of AzaC+atRa treatment on H3K27me3 and H3K9me3 levels**. T-HEp3 cells grown *in vitro* were treated with AzaC +atRA or PBS/DMSO as described in Fig. 4a were stained for the indicated markers and percent of high MFI cells scored.*p<0.05, unpaired t test. **c) AzaC+atRa treatment renders T-HEp3 cells [H3K27me3/H3K9me3/NR2F1/SOX9]^{high}*in vivo***. T-HEp3 cells were treated with AzaC+atRa as described in Supplementary Fig. 4f and 1 day after washout cells were inoculated into CAMs (150×10^3 cells/embryo). One-week later tumors were collected and histological sections were stained by IHC using the indicated antibodies. Scale bars, 50 μm. Insets show higher magnification views. Scale bars: 50 μm, insets= 15 μm. **d) NR2F1 is required to induce high H3K9me3 and H3K27me3 levels after AzaC+atRa treatment.** T-HEp3 cells were transfected with siControl or siNR2F1 and then treated with AzaC+atRA or PBS/DMSO as described in Supplementary Fig. 4f. 3 days after reprogramming cells were fixed and stained for the indicated markers. ***p<0.0005,

**p<0.005, *p<0.05, unpaired t test. Unless stated all data are representative of at least triplicate independent experiments, SD. For a, b and d, n=200 cells, y=percentage of cells with high MIF.

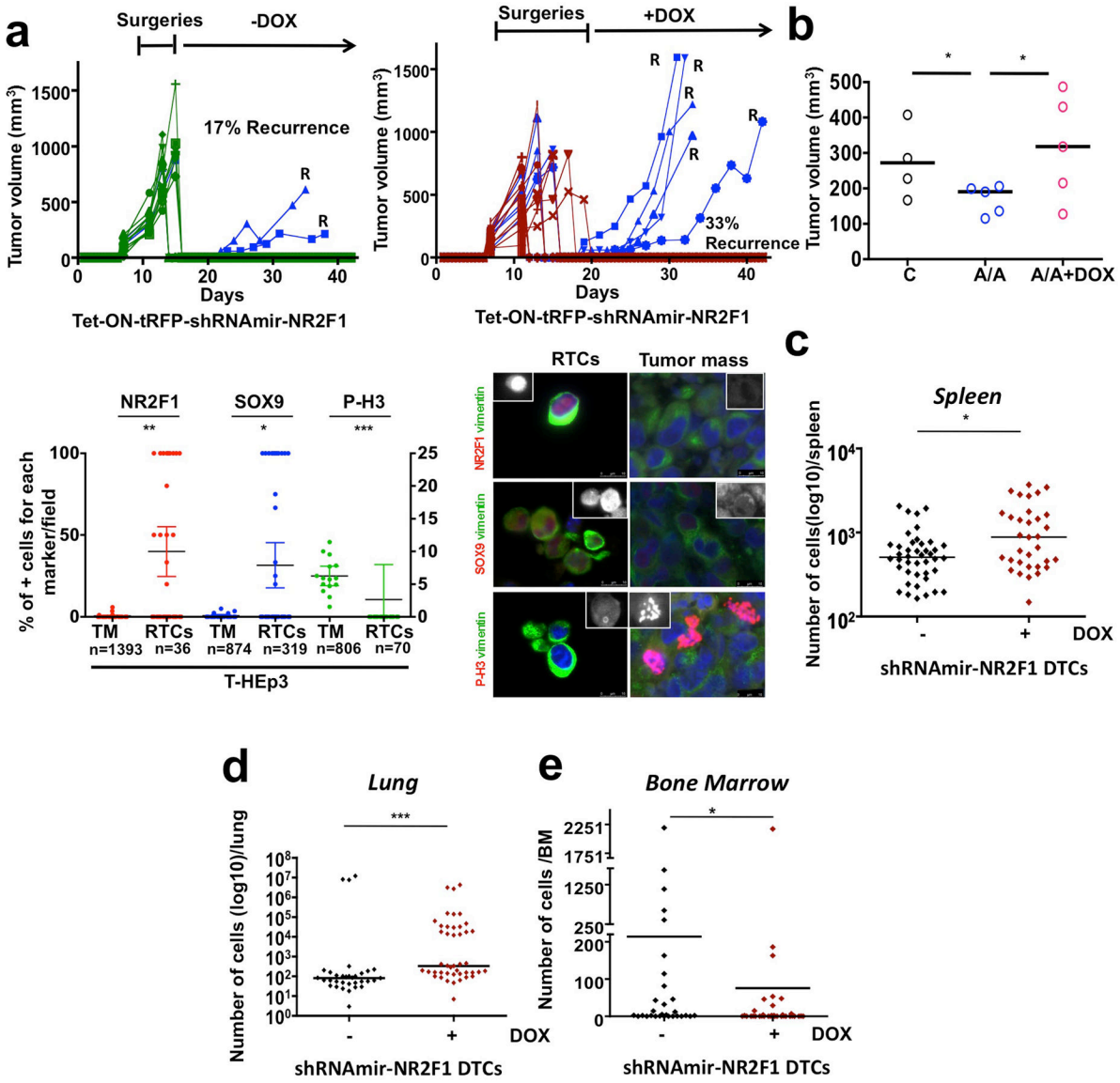

Figure 7. Effect of NR2F1 knockdown on loco-regional and distant recurrences

a) Upper panels: Tet-ON inducible shRNAmir-NR2F1 T-HEp3 cells s.c. tumors that reached ~800 mm^3 in nude mice were surgically removed and mice were treated with (25 mg/kg DOX, every 48 hrs., n=15) or without (N=12, middle panel) DOX (right panel). Flat green or red lines on the x-axis are all animals without recurrences. Lower left panel: skin sections in surgery margins (48 hrs. after surgeries) were analyzed by IF. T-HEp3 cells were identified by vimentin staining (green). NR2F1, SOX9 and P-H3 (red) were stained with specific antibodies. Graph = % of positive cells for each marker per field. TM=tumor mass, RTCs: single **r**esidual **t**umor **c**ells, n=total # of cells counted in 2–5 animals. The lower right panel shows representative pictures for each antigen. Inset: higher magnification of cells in the red channel (gray scale pseudo color). TM, n=3 animals, RTCs, n=3 animals; for SOX9: TM, n=3 animals, RTCs, n=5 animals; for P-H3: TM, n=2 animals, RTCs, n=3 animals. Bars: 10 μm. **b) NR2F1 knockdown and AzaC+atRA**(A/A)**-induced dormancy**. T-HEp3

cells treated *in vitro* with PBS/DMSO (c= control) or A/A treatment were inoculated into nude mice (n=5) and then treated as in (a); 12 days later tumor growth was measured. *p<0.05, unpaired t test. **c) Effect of NR2F1 knockdown on spleen DTCs**. DTCs isolated from spleen of the same animals in (a) were detected by Alu-QPCR as described[6] Mann Whitney test p<0.05. SPLEN DTCs: n=14 mice control, n=11 mice shNR2F1, y=ct values in triplicate per mice**. d) Effect of NR2F1 knockdown on lung DTCs**. The same animals in (a) were used to detect DTCs from lung by Alu-QPCR. Mann Whitney test p<0.05. lung DCTS: n=11 mice control, n=14 mice shNR2F1,y=ct values in triplicate per mice. **e) Effect of NR2F1 knockdown on BM DTCs.** BM aspirates from same animals in (a) were used to detect BM DTCs by Alu-QPCR. Mann Whitney test p<0.05. BM DTCs: n=10 mice control, n=12 mice shNR2F1 y=ct values in triplicate per mice. Unless stated all data are representative of at least duplicate independent experiments, SD.

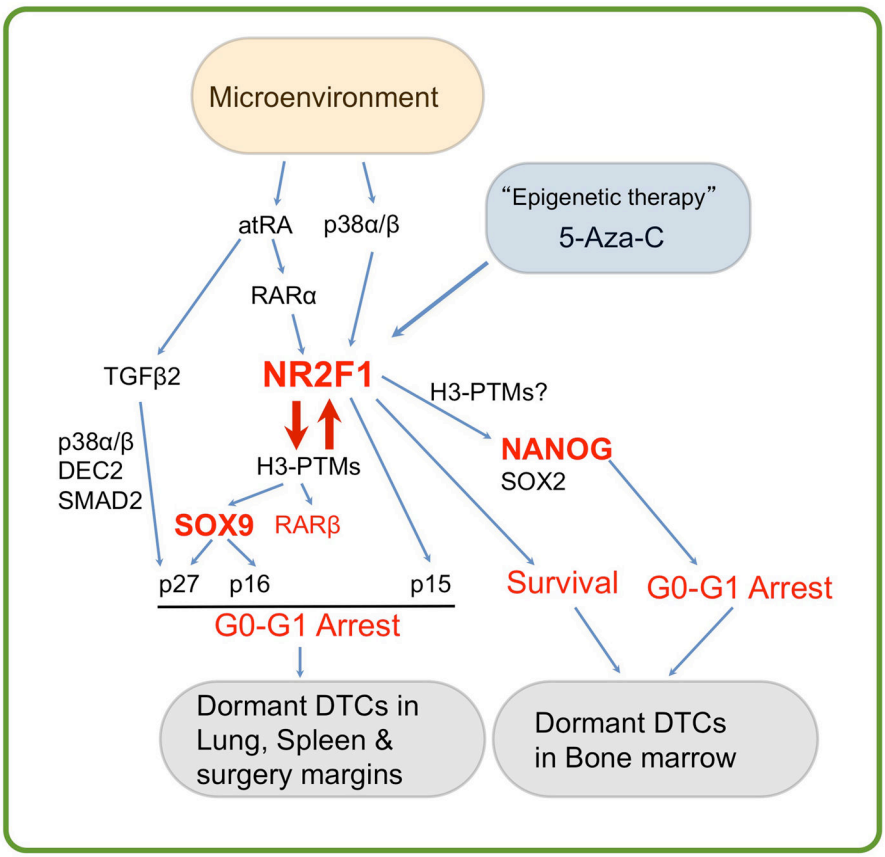

Figure 8. Integrative scheme of NR2F1 functions and the regulation of DTC fate

DTCs that arrive to specific microenvironments (e.g. lung, bone marrow) might integrate stress signals imposed by dissemination (p38α/β activation), by the new microenvironment and growth restrictive signals that maintain normal organ function (atRA+p38α/β activation). These signals jointly result in NR2F1 upregulation, which can in turn induce a quiescence program via the induction of CDK inhibitors (i.e. p16). This is executed by another set of TFs that include at least SOX9 and RARβ. In lung, spleen and surgery margins, the NR2F1-regulated quiescence program seems to be important to maintain dormancy, while in the bone marrow NR2F1 appeared to primarily regulate survival of DTCs. NR2F1 was also found to regulate the expression of two key pluripotency genes, NANOG and SOX2. A division of labor between NANOG and NR2F1 occurs in BM DTCs where growth arrest signals are regulated by NANOG while survival pathways are subjected to NRF21 functions. The ability of NR2F1 to coordinate these programs long-term may be due to its ability to generate global changes in histone H3 PTMs. atRA also regulates the induction of TGFβ2 in malignant cells that further induces signals in the dormancy program by inducing DEC2 *via* canonical and non canonical TGFβ2 signaling; this is independent of NR2F1. Finally, the dormancy program may be manipulated to favor dormancy maintenance using 5-Aza-C combined with atRA as an epigenetic therapy. This reprogramming protocol may also be used to study how dormant cells survive in quiescence and design anti-survival therapies that target quiescent DTCs.